

Delamination Detection in a Composite Plate using a Dual Piezoelectric Transducer Network

Chul Min Yeum^a, Hoon Sohn^{a*} and Jeong Beom Ihn^b

^aThe Department of Civil and Environmental Engineering, Korea Advanced Institute of Science and Technology, Daejeon 305-701, South Korea

^bBoeing Research & Technology, 9725 East Marginal Way South, Mail Code 42-25 Seattle, WA 98108, United States

ABSTRACT

In this study, a new damage detection technique is developed so that delamination in a multilayer composite plate can be detected by comparing pitch-catch Lamb wave signals in a piezoelectric transducer network rather than by comparing each signal with its corresponding baseline signal obtained from the pristine condition. The development of the proposed technique is based on the premise that the fundamental anti-symmetric mode (A_0) slows down when it passes through a delamination area while the speed of the fundamental symmetric mode (S_0) is invariant. First, the relative time delay of the A_0 mode in each path with respect to other paths is used as a delamination sensitive feature, and for extracting the delay feature of the A_0 mode, a new mode extraction technique is proposed. This mode extraction technique uses dual piezoelectric transducers composed of a concentric ring and circular piezoelectric transducers, and it is capable of isolating the A_0 mode in any desired frequency without frequency or transducer size tuning. Once the A_0 modes are extracted from all pitch-catch paths in the transducer network, a proposed instantaneous outlier analysis is performed to identify the wave propagation path(s) affected by the delaminated region(s). Because the relative time delays of the A_0 modes in the existing paths are instantaneously computed without using any reference data, it has been demonstrated that robust delamination detection can be achieved even under varying temperature conditions.

Keywords: Delamination detection, piezoelectric transducer network, Lamb wave, mode decomposition

1. INTRODUCTION

Structural health monitoring (SHM) is a process to evaluate and assure the safety and performance of structures. Recently, there have been increasing demands for SHM systems in the aerospace industry as composite materials are widely used in aircraft structures. Composite materials have many advantages over metals such as lightweight and superior specific strength and stiffness properties. However, the occurrence of damage due to abrupt impact or sequential accumulation of defects under fatigue loading during operation may considerably degrade structural strength or stiffness and severely reduce system reliability. Moreover, since most damages (e.g. delamination or debond) occur beneath the surface of composite structures, they are hardly visible or detectable. Therefore, the development of effective damage detection techniques has been needed to ensure performance and safety of composite materials.

Lamb wave based structural health monitoring (SHM) has gained a great amount of attention in the SHM of composite materials [1-4]. Lamb waves, which propagate in a solid plate with parallel free boundaries, are mechanical waves whose wavelengths are in the same order of magnitude as the thickness of the plate. The use of Lamb waves offers several advantages as a tool for damage detection and monitoring including (1) the inspection of large areas with little

* Corresponding author, hoonsohn@kaist.ac.kr; Tel. 82-42-350-3665; fax 82-42-350-5665

attenuation in a relatively short time, (2) excellent sensitivity to multiple defects like cracks, debonds or delaminations, and (3) the lack of needs for complicated and expensive insertion of radiation devices [3].

A great deal of theoretical and experimental works on the Lamb wave based delamination detection for composite materials has been reported in the literatures. First, in a pulse-echo configuration, reflection and/or scatter waves which are generated from delamination edges have been a good indicator for the delamination detection [5-7]. It is observed that phase delay and amplitude changes of these waves are closely related to the delamination size. Next, transmitted waves which pass through delamination areas have been analyzed in a pitch-catch configuration. Energy dissipation of the first arrival waves in delamination areas is commonly employed [8-9]. The time delay of a specific Lamb wave mode is also considered as a promising damage parameter for detecting and quantifying delamination [8]. Lastly, correlation analysis based damage detection algorithm has been proposed to minimize the false alarm coming from complex propagation characteristics of Lamb waves caused by damage and/or geometric complexities [10]. This algorithm only focuses on integrated changes between the present (with damage) and the reference signals (without damage) without the extraction of detailed damage signature.

These conventional techniques have commonly focused on the schemes where baseline signals are measured from the pristine condition so that changes from the baseline data can be detected and related to defects. However, large amount of the signal changes under varying environmental conditions like temperature mask the small signal changes due to damage, making damage detection challenging. Even if damage is detected, there exists a high rate of positive false alarms.

To overcome this problem, damage detection techniques which are insensitive to environmental effects such as temperature and load variations have been developed by relaxing the dependency on the prior baseline data [11-13]. However, the majority of works focus on the detection of crack or corrosion damages in metallic materials, and little is known about the detection of delamination in composite materials. In this study, a new delamination detection technique is proposed so that delamination can be detected without using any direct comparison with previously obtained baseline data even at the presence of temperature variations. The development of the proposed technique is based on the premise that the fundamental anti-symmetric mode (A_0) slows down when it passes through a delamination area while the speed of the fundamental symmetric mode (S_0) is invariant of delamination. Based on the delay of the A_0 mode in the delamination area, the existence of delamination can be identified by comparing the relative time delay of the A_0 mode in each path with respect to other paths without comparing one with its corresponding baseline signal obtained from the pristine condition. For the extraction of the A_0 mode in each path, a mode extraction technique using dual PZTs, which are composed of ring and circular PZTs, is proposed based on the mode decomposition technique developed by authors [14]. Once the relative time delay of the A_0 modes in all existing paths are computed, a proposed instantaneous outlier analysis is conducted so that a damage threshold for damage diagnosis can be automatically calculated only using current data.

The effectiveness of the proposed technique is experimentally validated under temperature variations using a simple composite specimen. Additionally, the capability of the proposed technique in a complex geometric composite structure is evaluated using a complex composite specimen with stringers. The advantages of this technique are (1) robust delamination diagnosis even under varying temperature using an automatically determined damage threshold, (2) effective detection of multiple delaminations, and (3) application to complex geometric structures by applying the proposed mode extraction technique using dual PZTs.

This paper is organized as follows. In Section 2, the effects of delamination and temperature on Lamb wave modes are investigated. In Sections 3 and 4, the mode extraction technique and delamination detection algorithm are proposed, respectively. The potential and robustness of the proposed technique are illustrated by experimental studies presented in Section 5. In Section 6, application of the proposed technique to a complex composite structure with stringers is investigated, and followed by the conclusion in Section 7.

2. THE EFFECTS OF DELAMINATION AND TEMPERATURE ON LAMB WAVE MODES

Lamb waves are highly dispersive and multimodal waves. When Lamb wave modes encounter defects along its wave propagation path, the wave reflects, scatters and converts into different types of modes. Newly created and/or existed

multiple Lamb wave modes are overlapped each other in the time or frequency domains. To make matters worse, they are independently fluctuated and shifted due to continuously varying environmental conditions like temperature. In real applications, since these adverse characteristics of Lamb waves often mask subtle structural changes caused by damage, followed by lots of false alarms in the damage diagnosis, the appropriate selections of Lamb wave modes and features sensitive to damage but insensitive to environmental variations are crucial.

The authors first examine the effects of delamination and temperature on Lamb wave modes for the development of robust damage detection techniques. Regarding the effects of delamination and temperature, the findings from numerical and experimental studies are represented as follow. First, through experimental tests, it is shown that the A_0 mode slows down when it passes through a delamination area while the speed of the S_0 mode does not change much at delamination. Furthermore, a proportional relationship between the severity of delamination and the time delay of the A_0 mode is observed. As for the amplitude of the A_0 mode, initially, the delamination causes a little amplification of the A_0 mode, followed by attenuation with further increases of the degree of delamination. Although these results are unexpected, other researches have also found the A_0 mode attenuation but initial amplification [8, 13]. The distortion of the A_0 or S_0 mode waveform is hardly observed. Numerical simulation also reveals that the A_0 mode is more significantly delayed and attenuated by delamination than the S_0 mode. This is because delamination primarily decreases interlinear shear strength. Figure 1(a) shows that the A_0 mode is delayed and attenuated due to delamination, when Lamb wave signals measured from the undamaged and delamination conditions of a composite specimen are compared. Additionally, it is concluded that mode conversion occurs due to delamination, but the converted modes rapidly attenuate, making it practically challenging to reliably measure converted modes. In numerical simulation, the amplitude of converted modes due to a typical delamination was less than 1% of the amplitudes of the fundamental symmetric and anti-symmetric modes.

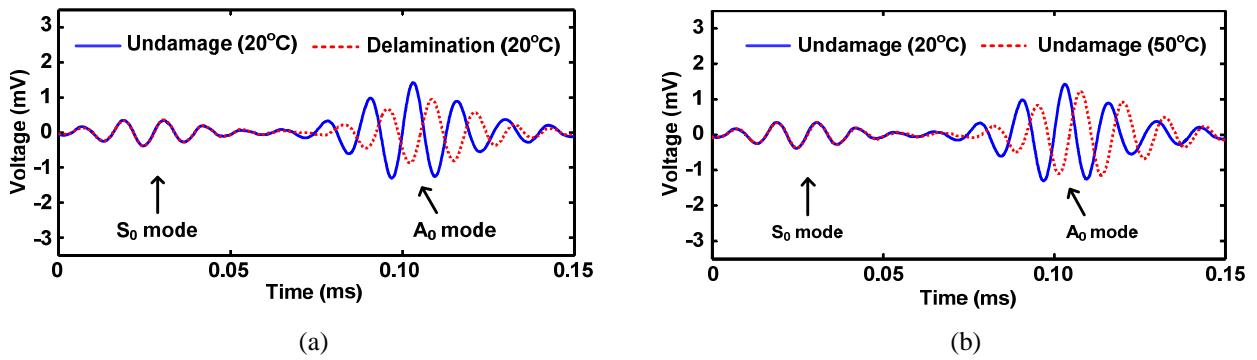


Figure 1. Similar effects of delamination and temperature on Lamb wave modes in a composite specimen (Both delamination and temperature cause time delay and attenuation of the A_0 mode): (a) Delamination effects and (b) Temperature effects (The solid lines are measured at 20°C under the undamaged condition. The dashed lines in (a) and (b) are obtained at 20°C under the damaged condition and at the 50°C under the undamaged condition, respectively.)

Next, the effect of temperature on Lamb wave modes is investigated. Similar to the effect of delamination, the amplitude and arrival time of the A_0 mode are affected by temperature variations. More specifically, as shown in Figure 1(b), it is observed that as temperature increases, the A_0 mode amplitude decreases and the arrival time of the A_0 mode is delayed. However, the S_0 mode characteristics are rarely affected by temperature.

These results show the practical limitations of the conventional damage detection techniques, which may occur in field applications. Because of the similar effects of delamination and temperature on Lamb wave modes, it is difficult to infer the damage state of a structure by comparing the current data with the baseline data under temperature variations. To address this issue, in this study a delamination detection technique, which does not rely on previously obtained baseline data and can be easily automated, is proposed for robust delamination detection in composite materials. Since the proposed technique is based on the time delay of the A_0 mode due to delamination, it is necessary to isolate the A_0 mode from the undesired S_0 mode. Next section, the mode extraction technique, which can isolate the A_0 mode, is firstly introduced.

3. LAMB WAVE MODE EXTRACTION TECHNIQUE

As mentioned in the previous section, it is desirable to use the A_0 mode for the delamination detection because the A_0 mode is more sensitive to delamination than the S_0 mode. However, due to the co-existence of the S_0 and A_0 modes and multiple reflections from structural boundaries, the extraction of delamination features, which is only included in the A_0 mode, may be difficult without isolating one from measured signals. Thus, the Lamb wave mode extraction technique is proposed using dual PZTs in this study.

The proposed mode extraction technique is formulated based on the previous developed mode decomposition technique by authors. The previous mode decomposition technique decomposes S_0 and A_0 modes from measured signals. However, due to the fast velocity of the S_0 mode in composite materials compared to that in metallic materials, it is hard to compute the “scaling factors” from tested or existing reference paths, which is necessary for the mode decomposition [14]. Instead of decomposing the S_0 and A_0 modes, the proposed A_0 mode extraction technique isolates only the A_0 mode wave packet having arbitrary amplitude without computing the “scaling factors”.

The advantages of the proposed mode extraction technique have (1) PZTs need to be placed only a single surface of a structure, (2) mode extraction can be performed at any desired frequency without physical adjustment of the PZT size and/or spacing, and (3) a circular design of the dual PZT allows omni-directional A_0 mode extraction.

3.1 Descriptions of the dual PZT and signal notations

First, the configuration of a dual PZT which is used for the A_0 mode extraction is presented. Figure 2 shows the schematic drawing of the dual PZT. The dual PZT consists of a concentric ring and circular PZTs. These two components can be activated independently for Lamb wave excitation and sensing [12, 15].

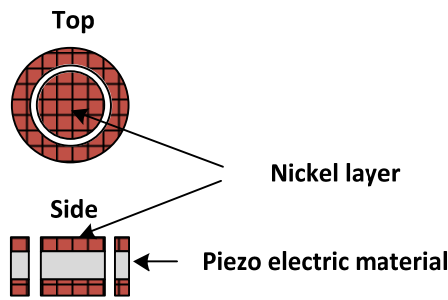


Figure 2. A schematic drawing of the dual PZT composed of co-centered ring and circular PZTs

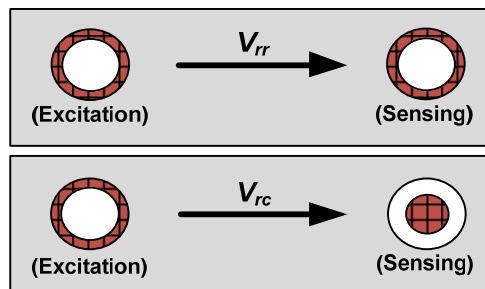


Figure 3. Notations of signals obtained from the dual PZTs: V_{rr} denotes a response measured by the ring part of the sensing PZT when the ring part of the exciting PZT is activated. Similarly, V_{rc} is measured by the circular part of the sensing PZT when the ring part of the excitation PZT is actuated. The darker (red) area of the dual PZT represents the PZT component activated either for excitation or sensing.

By activating ring and circular parts of the excitation and sensing dual PZTs, four different Lamb wave signals can be obtained: V_{ij} , i and $j = r$ and c . Here, i and j denote the areas of the dual PZTs activated for excitation and sensing, respectively: r and c represent the ring and circular parts of the dual PZT. For example, V_{rr} represents a response signals

measured by the ring part of the sensing dual PZT when the ring part of the excitation dual PZT is activated. V_{rc} is defined in a similar manner. The darker (red) areas in Figure 3 show the PZT parts activated for either Lamb wave excitation or sensing.

3.2 A theoretical Lamb wave propagation model using circular PZTs

The proposed mode extraction technique is based on an analytical solution of the Lamb wave propagation modeling using 3D circular PZT actuation and sensing. One pair of circular PZTs mounted on the surface of an isotropic structure is used as an actuator and a sensor in pitch-catch mode. The circular PZT actuation was modeled as causing in-plane traction on the plate surface along its free edge and the output response was derived by integrating the strain over the sensing PZT. The ring PZT, which is a part of the dual PZT, was also modeled as actuator and sensor using the theoretical circular PZT model [14].

The derived theoretical Lamb wave propagation solution gives three key features, which are necessary for the mode extraction technique, presents as follows:

- (1) The Lamb wave modes measured at the circular and ring parts of the dual PZT have identical arrival times but different amplitudes (same principle applies for exciting Lamb wave modes).
- (2) The amplitudes of the S_0 and A_0 modes change at “different” rates, as the sizes of exciting and/or sensing PZTs vary.
- (3) The amplitude change rate of each mode with respect to the PZT size is independent of the wave propagation distance.

For example, the S_0 modes in V_{rr} and V_{rs} have identical arrival times but different amplitudes. The amplitude ratio of the S_0 mode in V_{rr} to that in V_{rs} is different from the amplitude ratio of the A_0 mode in V_{rr} to that in V_{rs} because V_{rr} and V_{rs} are measured at the different size of the sensing PZTs (ring and circular PZTs). The amplitude ratio of the S_0 mode in V_{rr} to that in V_{rs} does not change regardless of whether the amplitude of the S_0 mode is taken from the first arrival signal or reflection signals or overlapped both signals, because the amplitude ratio is independent of the wave propagation distance of the S_0 mode. Since the amplitude ratio of the S_0 modes is not identical with that of A_0 modes, the A_0 mode can be extracted by simply subtracting V_{rr} from V_{rs} after normalizing V_{rr} and V_{rs} with the amplitudes of the S_0 modes in each corresponding signal.

3.3 Procedure for the proposed mode extraction technique

The procedure of the proposed mode extraction technique is summarized as follows:

- (1) V_{rr} and V_{rs} are measured at ring and circular parts of sensing PZTs by actuating the ring part of an exciting dual PZT.
- (2) The amplitudes of the S_0 modes in V_{rr} and V_{rs} are normalized so that the S_0 mode amplitudes are equal and then the S_0 modes are removed by subtracting V_{rr} from V_{rs} .
- (3) The extracted signal is filtered using a matching pursuit technique to increase the signal to noise ratio.
- (4) Finally, the A_0 mode wave packet with arbitrary amplitude can be extracted.

Here, instead of V_{rr} and V_{rs} , a pair of V_{ss} and V_{sr} , V_{rr} and V_{sr} or V_{rr} and V_{ss} can be also used for this technique. Note that the amplitude of the S_0 mode can be taken from the amplitude of V_{ij} at arbitrary same time before the first arrival A_0 mode reaches. The extracted A_0 mode wave packets include the time of flight information and thus, the time delay feature can be identified by comparing those in other undamaged paths, even if the extracted A_0 mode wave packets do not preserve the amplitude information of the A_0 modes in V_{rr} and V_{rs} .

The analytic solution of the Lamb wave propagation model used in this technique is derived in the undamaged condition of a structure [14]. Even so, the A_0 mode can be effectively extracted from measured signals in the presence of delamination because (1) the wave packets of the A_0 and S_0 modes are not much distorted due to delamination, and (2) the S_0 mode is rarely affected by the delamination and thus the amplitude ratio computed using the first arrival S_0 mode that passes through delamination is not much changed compared with that computed using S_0 mode reflections from boundaries.

4. LAMB WAVE MODE EXTRACTION TECHNIQUE

Uniquely takes advantage of the fact that delamination in composite materials causes mainly the time delay of the A_0 mode without changing the S_0 mode, an instantaneous delamination detection technique is developed. This technique detects delamination within a dual PZT network by instantaneously comparing the time of flights of the A_0 modes

obtained from multi-path pitch-catch Lamb wave signals. The term of ‘instantaneously’ describes that damage detection can be made only using the ‘current state’ data without relying on pre-recorded ‘baseline’ data from the undamaged conditions. In this way, susceptibility to false alarms due to operational and environmental variations of the structure is minimized.

The detailed procedure of the proposed damage detection, shown in Figure 4, is as follow. First, Lamb wave signals are obtained from multiple actuator-sensor combinations in the dual PZT network. A dual PZT, which is composed of a concentric ring and circular PZTs, is used for the A_0 mode extraction. An array of dual PZTs is placed on one of a surface of the structure so that actuator-sensor paths are of equal spacing and angle. Then, the first arrival of the A_0 mode is extracted from signals in each path in the dual PZT network using the proposed mode extraction technique. Using the extracted A_0 modes in all paths, a damage index in each path, which is sensitive to the time delay of the A_0 mode caused by delamination, is computed. Finally, when the A_0 mode of a specific path becomes significantly slower than these of the other paths, it is diagnosed that a delamination is along that specific path. Here, for the robust damage classification without using baseline data, instantaneous outlier analysis has been developed.

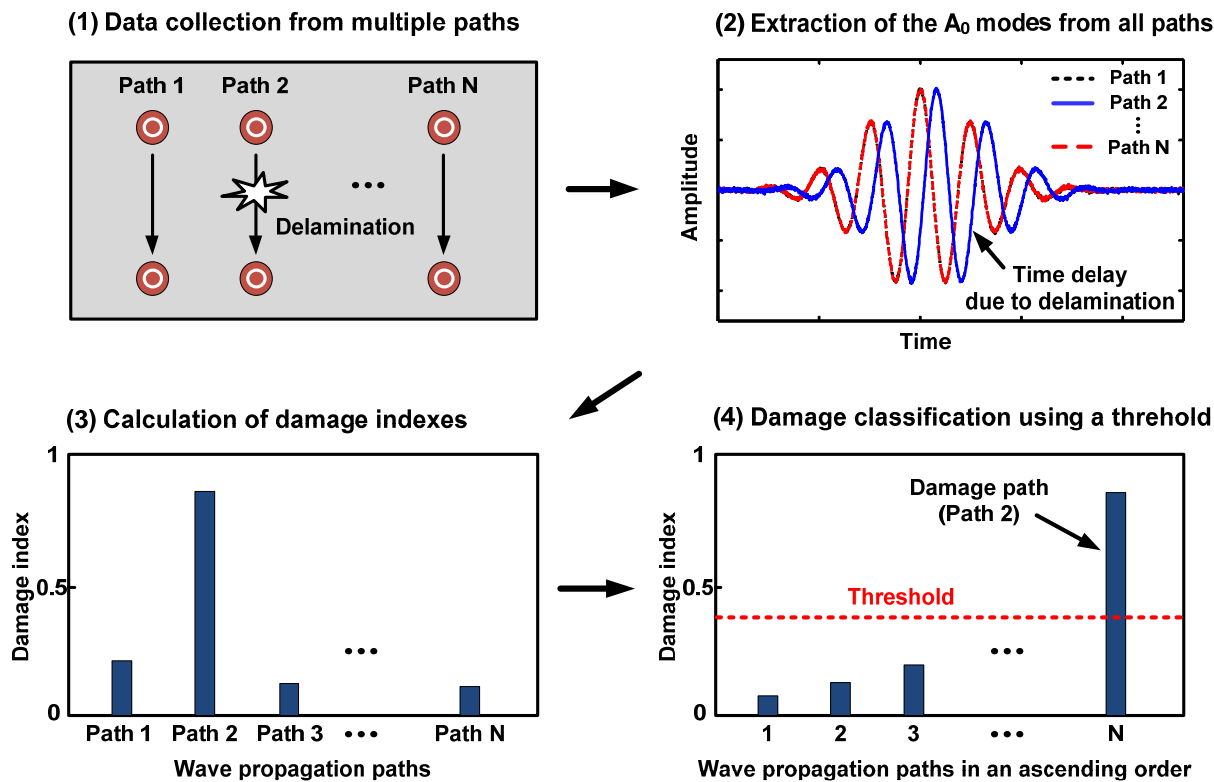


Figure 4. Overall procedure of the proposed instantaneous damage detection technique: (1) Collection of Lamb wave signals from the dual PZT network on the composite structure (actuator-sensor paths are installed with equal spacing and angle), (2) Extraction of the A_0 mode from all wave propagation paths using the proposed mode extraction technique, (3) Calculation of damage indexes which indicate the time delay of the A_0 mode caused by delamination, and (4) Classification of damage paths using proposed instantaneous outlier analysis (The threshold is automatically determined only using current damage indexes)

The proposed delamination detection technique identifies damaged path(s) by comparing the first arrival A_0 modes obtained from paths having an equal spacing and angle. Since the arrival times and amplitudes of the S_0 and A_0 modes are almost identical among these paths, a specific path affected by delamination can be easily estimated. However, the problem is, depending on path locations on the structure, different multiple reflections from structural boundaries and geometric features like stringers or joints are overlapped with the A_0 mode, making the comparison of the A_0 modes challenging. Furthermore, in composite materials, the S_0 mode reflections are easily overlapped with the first arrival A_0

mode compared to those in the metal because they have faster S_0 mode and slower A_0 mode [3]. For direct comparison of the A_0 modes in all paths, it is needed to apply the mode extraction technique to the proposed delamination detection technique.

4.1 Data collection

An array of PZTs is installed on the composite structure for delamination detection and localization. Each PZT acts as both an actuator and a sensor for Lamb wave excitation and sensing. One PZT is designated as an actuator, exerting a predefined toneburst waveform into the structure. Then, the adjacent PZTs measure the response signals. This process, called as the pitch-catch Lamb wave sensing mode, is repeated to different wave propagation paths. The wave propagation paths are divided into groups and each group consists of paths having same spacing and angle for comparing the time of flight of the A_0 modes among these paths. For increasing delamination detectability and estimating exact location(s), each group has enough wave propagation paths to be compared each other.

4.2 Damage index

For identifying the presence of delamination in the monitoring area, the cross-correlation based delamination detection technique is introduced. As mentioned previously, delamination in composite materials causes the time delay of the A_0 mode without changing the S_0 mode. Based on this observation, a damage index is defined to capture the time delay of the A_0 mode by computing a cross-correlation between the A_0 modes in a test path and undamaged paths. The basic assumption of the proposed damage index is that more than half of paths in the group, which consists of paths having same spacing and angle, are collected from the undamaged condition. The definition of the damage index (DI) is as follow in Eqs. (1) and (2).

$$DI(i, \Omega) = \frac{1}{2} \left(1 - \frac{2}{n_d} \sum_j^{n_d/2} \text{corr}(A_0(i, \Omega), A_0(j, \Omega)) \right) \quad (1)$$

$$DI(i) = \frac{1}{N} \sum_{\Omega}^N DI(i, \Omega) \quad (2)$$

where corr is the cross-correlation, Ω is the input frequency, path i is the test path, d is the group number of the paths i and j , and n_d is the number of paths in the group d . $A_0(i, \Omega)$ and $A_0(j, \Omega)$ are the first arrival A_0 modes at the frequency Ω in the paths i and j , respectively. The path j is the undamaged path having same spacing and angle with the path i . The undamaged paths (path j) are selected as the half of the fastest A_0 modes in the group d . The DI value of the path i is denoted $DI(i)$, which is averaged over N different frequencies in Eq. (2).

The DI value expresses how much a test path is delayed compared with undamaged paths. The proposed DI is insensitive to the attenuation or amplification of signals because the cross-correlation analysis confirms the linear relationship between two signals. The DI value falls on 0 to 1 by subtracting the cross-correlation values from one and dividing it with 2. If the A_0 mode obtained from a test path has similar arrival time with those from assumed undamaged paths, the DI value approaches to 0. Otherwise, if the A_0 mode is delayed due to delamination, corresponding DI value goes to 1. Note that due to periodical toneburst waveform, if the time delay of the A_0 mode due to delamination occurs more than half period of the A_0 mode waveform in time domain, the DI value starts to decrease even under increasing the degree of delamination. However, in the preliminary experimental tests, before the A_0 mode is delayed more than half period of the A_0 mode waveform in time domain, the A_0 mode is almost attenuated and much distorted due to severe delamination. In this case, the time delay based proposed delamination detection technique is limited to be applied.

4.3 Instantaneous outlier analysis

After computing DI values in all paths, damage classification is conducted. Once a DI value in a specific path exceeds a threshold value, the corresponding path is defined as damaged. However, the critical problem is how to determine the threshold value so that damaged path are properly detected without misclassification. The common practice has been to collect the DI values from the baseline condition of a structure and to characterize the distribution of the DI values. Once the distribution of the DI value is properly estimated, a threshold value can be established for a user-specified confidence level. However, as mentioned in the introduction, predetermined decision boundaries obtained from baseline data may falsely indicate damage or allow damage to go undetected in the presence of varying environmental conditions like temperature. In this study, the instantaneous outlier analysis is proposed to automatically detect damaged path(s) among

all possible wave propagation paths in the PZT network without using predetermined threshold values or baseline data.

The procedure of the proposed damage classification is summarized as follow.

- (1) Calculate a DI value, which can estimate the time delay of the A_0 mode, for each path.
- (2) Arrange all DI values in an ascending order (1th index: the smallest and N^{th} index: the largest).
- (3) Fit a parametric distribution function to the $n-1$ smallest DI values, and compute a threshold corresponding to a specific confidence level defined by the end user. Here, the initial n is typically the half of the available path number.
- (4) If the value of the n^{th} smallest DI value is larger than the threshold value, the PZT paths associated with the n^{th} , $n+1^{\text{th}}$... N^{th} indices are determined to be damage. If not, repeat steps (3) and (4) for the next smallest value ($n+1$) until n reaches N .

For a parametric distribution function, a truncated exponential distribution which is one of bounded distribution is used because the DI value has the fixed upper (1) and lower (0) limits. A truncated exponential distribution with parameter c has the following probability density function [17]:

$$f(x) = ce^{-cx} (1 - e^{-c})^{-1}, \quad (0 < x \leq 1) \quad (3)$$

The maximum likelihood estimator of c , denoted c_b in Eq. (4), can estimate a parameter c of the best-fit truncated exponential distribution of x

$$\bar{x} = 1/c_b - 1/(e^{c_b} - 1) \quad (4)$$

where \bar{x} is the mean of x .

5. DELAMINATION DETECTION IN A SIMPLE COMPOSITE SPECIMEN

5.1 Description of the experimental set-up

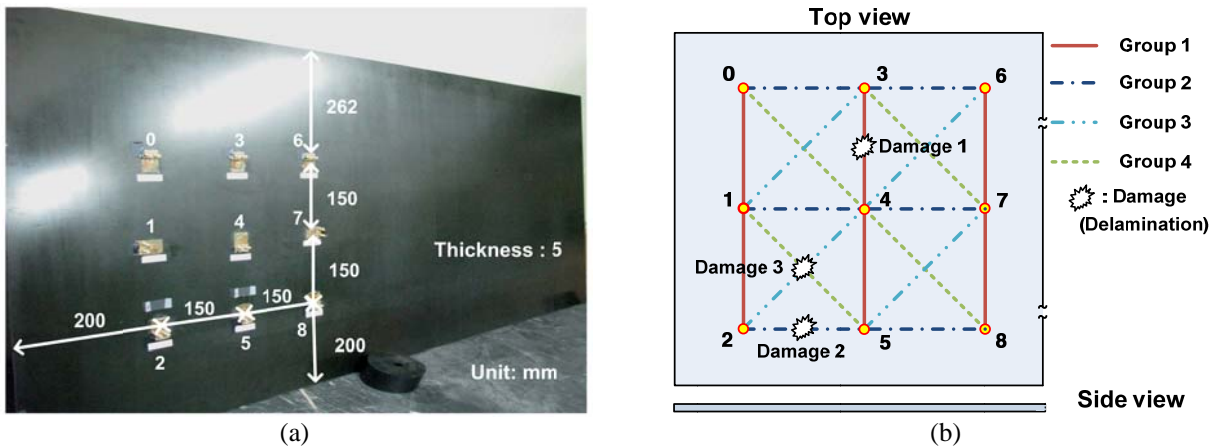


Figure 5. Experimental setup of a simple composite specimen: (a) A layout of the dual PZT network for data collection and (b) delamination locations and data collection paths (A total of 20 data collection paths with four different groups having same spacing and angle are investigated for damage detection and localization)

To validate the proposed delamination detection technique, a carbon fiber composite specimen is tested as shown in Figure 5(a). The dimension of the specimen is $1512\text{mm} \times 762\text{mm} \times 5\text{mm}$, and 9 dual PZTs are installed on the inside surface of the specimen in a square grid pattern with 15cm spacing. There are no complex geometric features such as ribs, stringer or curved surfaces. This specimen has unknown sequence and material properties, provided Boeing Company. The corners of specimens were supported on rubbers during the tests. A total of 20 paths are divided into 4 different groups that have equal spacings and angles. For example, four paths with 15cm spacing and aligned to 90 degree, red

solid lines in Figure 5(b), are included in the 'Group 1'. The long spacing paths like 2-7 or 2-3 path cannot be considered in this layout due to the lack of paths in a group to be compared. If a bigger array like 4 by 4 is installed on the specimen, various spacings and angles of paths can be considered.

A packing dual PZT composed of separated ring and circular PZTs (the radius of the inner ring, outer ring, and circular PZTs: 3mm, 4mm and 2mm) is used. This is to electrically isolate the dual PZT from the host structure and make wire connections easier [15]. Each dual PZT acts as both a sensor and an actuator for excitation and sensing of Lamb waves. Great care was taken to maintain a constant distance between PZTs for the exact estimation of the time delay. The only requirement of sensor placement is to decide the proper distance between the structural boundaries and PZTs to separate the first arrival A_0 mode with its reflections from boundaries. However this constraint is not significant in composite materials due to sufficiently slow velocity of the A_0 mode.

Low velocity impact damage(s) is(are) induced on the test area of the specimen using a conventional drop-weight impact tester with a 1cm radius steel ball tip. The impacts were applied to the same point three consecutive times with a constant energy of 24.5J. Three damages are introduced in the middle of 4-3 path, 2-5 path and the intersection of 2-4 and 1-5 paths, respectively, and the Lamb wave signals are measured as increasing the number of delamination.

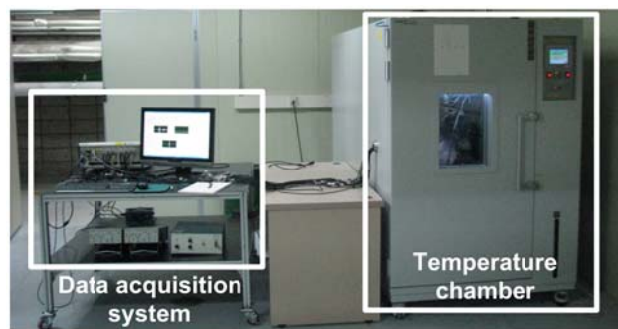


Figure 6. Experimental step for data acquisition and temperature tests

Figure 6 shows the overall test configuration. The damage acquisition system consists of an arbitrary waveform generator (AWG), a high speed signals digitizer (DIG), a low noise preamplifier (LNP), a power amplifier and multiplexers. Using the 14-bit AWG, a toneburst signal with a 10 peak to peak voltage was generated and amplified three times at the power amplifier, and then applied. The output voltage was filtered and amplified 50 times by the LNP, and measured by the DIG of which sampling rate and resolution was 20ms/s and 16 bits, respectively. The response signals were measured twenty times and averaged in the time domain to improve the signal to noise ratio. In the preliminary test, Lamb wave signals were obtained from one of distributed wave propagation paths to decide the input frequency range. Based on the measure signals, the input frequency range is set to 80 kHz ~ 120 kHz with 10kHz interval, which is below the cutoff frequency of A_1 and S_1 mods and relatively dominant of the A_0 mode. Since the best operated input frequency is changeable under varying environmental conditions and/or delamination sizes, the use of the board frequency range is advantageous to obtain the robust delamination detection results.

Another temperature experiments were conducted in each delamination condition using a temperature chamber. The testing temperature is set to -10, 20 and 50 °C. The 20 °C represents as the room temperature. A broader spectrum of temperature variations was not examined using the undamaged specimen to avoid any potential damage to the PZTs before performing subsequent delamination tests.

5.2 Test results

First, the effects of temperature and delamination on Lamb wave modes are investigated. By comparing of Lamb wave signals measured from the undamaged and delamination conditions, it is observed that the A_0 mode slows down and attenuates when it passes through a delamination area shown in Figure 1 (a). Similarly, the A_0 mode is attenuated and delayed as temperature increases shown in Figure 1 (b). On the other hand, in both cases, the S_0 mode does not change much at delamination and temperature variations. These similar effects of delamination and temperature prove that the use of baseline data for delamination detection may falsely indicate delamination or allow delamination undetected. Note

that Lamb wave signals used in Figure 1 are obtained from the path 4-3 in the specimen at an input frequency of 100 kHz.

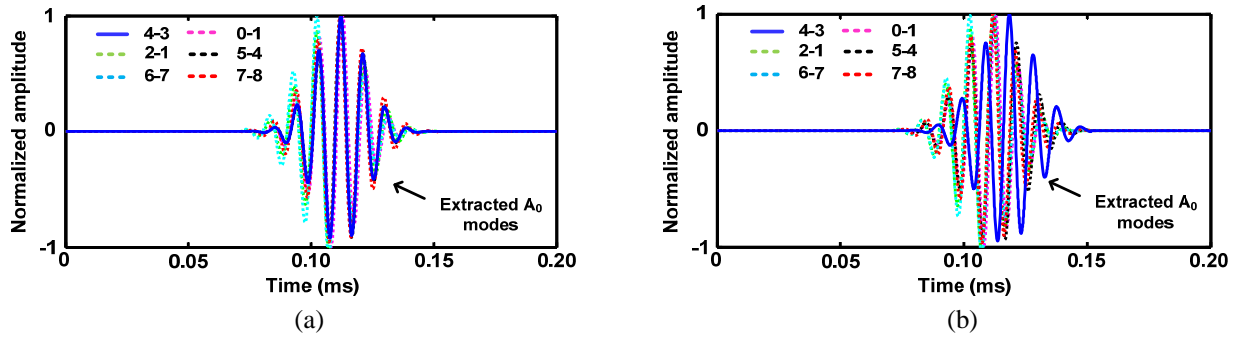


Figure 7. Comparison of the extracted A_0 modes in a group of paths: (a) Undamaged condition and (b) Damaged condition (The A_0 modes are extracted from paths in the group 2 on the simple composite specimen at 50°C and the matching pursuit technique is used for a noise filtering. Delamination is placed in the middle of the 4-3 path, marked as a solid blue line)

Figure 7 shows the comparison of the extracted A_0 modes in a same group before and after delamination. The A_0 modes used in this figure are extracted from the paths including the group 1 in Figure 5 (b) and obtained at a temperature of 50°C . By applying a matching-pursuit filtering, the only A_0 mode wave packets are left without any noise components. In Figure 7(a), the A_0 modes obtained from the initial undamaged conditions reveal consistent arrival time without any time delay. Otherwise, as shown in Figure 7(b), while the A_0 modes from undamaged paths still consistently arrive at the identical time (the dashed lines), one of the A_0 modes obtained from damaged condition, 4-3 path, exhibits the clear time delay (the blue solid line). This phase delay among paths is used for the damage indicator.

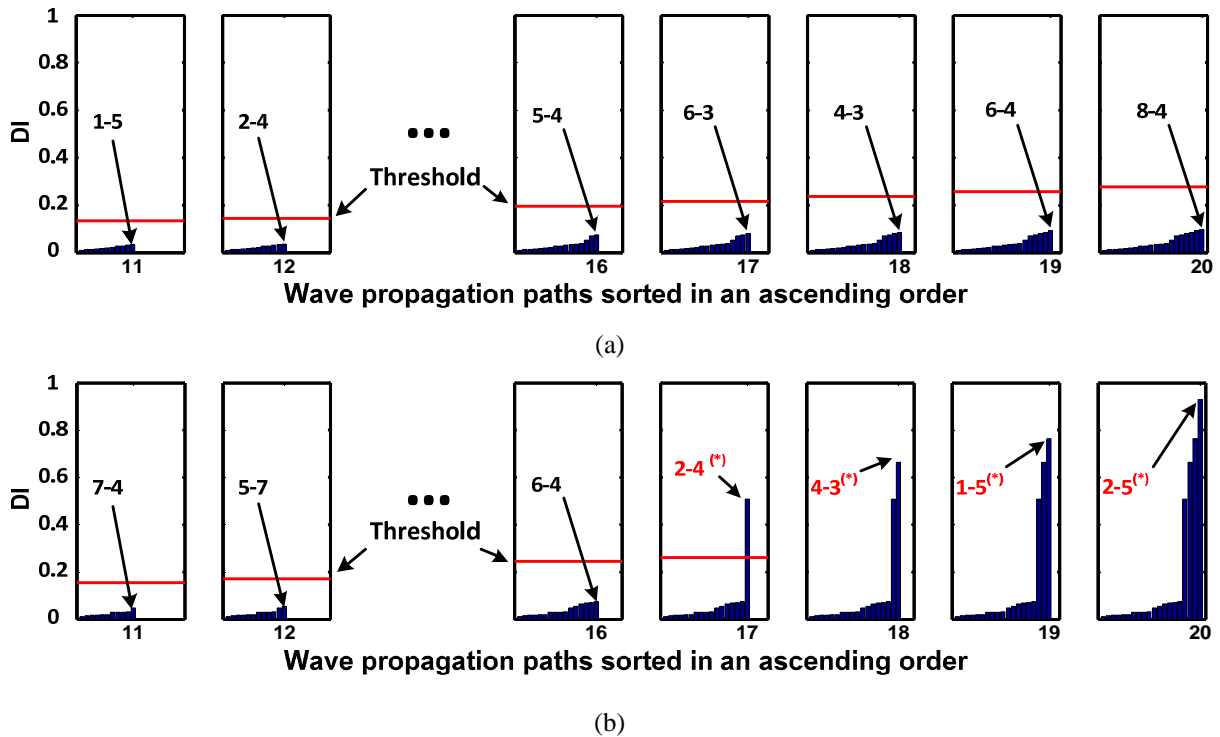


Figure 8. Examples of the instantaneous outlier analysis using an automated determined threshold: (a) Undamaged condition and (b) Delamination condition (A threshold is repeatedly determined until the DI of the test path is larger than the threshold. '*' is the detected damage paths.)

Figure 8 shows the graphical representation of the proposed instantaneous outlier analysis. The damage indexes (blue bars) used in this example are obtained at 50°C under the undamaged condition in Figure 8 (a) and under the damaged condition in Figure 8 (b). A pair of numbers in the each graph indicates the test path and the number below the graph indicates the order corresponding to the test path, when all paths are sorted in the ascending order. A threshold (red solid line) of the test path n is determined by fitting a truncated exponential distribution to the $n-1$ smallest DI value, and computing a one-sided 99.9% confidence interval. Since a total available path number is 20, the initial n start from 11th order. If the DI value of the test path is larger than the threshold value, the path(s) which have(has) the larger DI value than the test path's one is(are) determined to be damaged path(s). If not, the test path of the next smallest order is tested in the same until the test path become the largest order. In Figure 8 (a), the DI value of each test path is lower than the corresponding threshold value, and this case is classified into the undamaged condition. However, in Figure 8(b), the damaged path is firstly captured in the 16th order, and thus, the paths of the larger order than 17th are also determined as damaged paths.

All damage diagnosis results were summarized in Table 1. There are four cases depending on the number of introduced delaminations on the specimen. Each case has been examined under three different temperatures (-10, 20 and 50°C) to investigate if the proposed delamination classifier would be robust under varying temperature. As a result, the number of introduced delamination and corresponding paths are successfully detected using the proposed instantaneous outlier analysis. Additionally, undamaged paths are no The important results that are not included in Table 1 are that the detected paths are only damaged paths. Even under high (50°C) and low (-10°C) temperatures, no indication of delamination was provided in the undamaged condition. Note that the threshold values in the cases 1, 2 and 3 indicate the initial threshold that the paths are firstly detected as damage, and those in the case 1 are the one that is used to test the largest DI value

Table 1. Instantaneous delamination detection under changing temperatures

Case	Damaged location(s)	Temp. (°C)	Threshold value	Damaged path(s) (DI value)	Damage diagnosis
1	0 (Undamage)	-10	0.164	None	Any path is not classified as damage.
		20	0.247	None	
		50	0.276	None	
2	1 (Damage 1)	-10	0.176	4-3(0.674)	A damaged path is detected.
		20	0.262	4-3(0.842)	
		50	0.285	4-3(0.702)	
3	2 (Damages 1,2)	-10	0.189	4-3(0.693), 2-5(0.923)	All damaged paths are detected.
		20	0.274	4-3(0.778), 2-5(0.875)	
		50	0.266	4-3(0.725), 2-5(0.926)	
4	3 (Damages 1,2,3)	-10	0.147	2-4(0.375), 4-3(0.647) 1-5(0.807), 2-5(0.921)	All damaged paths are detected.
		20	0.279	2-4(0.339), 4-3(0.737) 1-5(0.841), 2-5(0.862)	
		50	0.261	2-4(0.508), 4-3(0.663) 1-5(0.764), 2-5(0.930)	

Additionally, the Kolmogorov-Smirnov (K-S) test is conducted to make sure if a truncated exponential distribution is properly selected as an empirical distribution of DI values obtained from undamaged specimens. In statistics, the K-S test about the one-sample case is used to check whether the sample is drawn from the reference distribution. This test is a nonparametric method, and it does not depend on tested empirical distribution. After estimating a parameter for a truncated exponential parameter using Eq. (6), reference distribution can be obtained based on the estimated parameter and then, the K-S test check whether the DI values obtained from undamaged specimens follows the reference distribution. In this study, MATLAB software is used to compute, and the results are that all DI values obtained from the undamaged conditions follow the assumed truncated exponential distribution. Thus, it turns out that the use of the truncated exponential distribution is proper for the proposed instantaneous outlier analysis.

6. CONCLUSION

In this study, a new instantaneous delamination detection technique is developed which explicitly considers the effects of varying environmental conditions without using any direct comparison with baseline data obtained from undamaged conditions. The interaction characteristics of Lamb waves with delamination are experimentally examined. Then, features sensitive to delamination but insensitive to ambient operational environmental variations of a composite structure for detection of delamination are identified. Third, specific PZT transducer designs and signal processing techniques are proposed to isolate the damage sensitive feature from measured Lamb wave signals. Finally, instantaneous damage classification techniques, which operate on the extracted features, are developed so that the existence of defects can be identified and classified. The effectiveness of the proposed technique is experimentally demonstrated explicitly under varying temperature. However, it should be noted that the proposed technique best operates under the following conditions: (1) The more paths having identical spacing and angle are installed, the more exact delamination detection and localization results can be obtained, (2) All the dual PZTs installed are identical in terms of their size and a fixed spacing, (3) The driving frequency is selected so that only the S_0 and A_0 modes are excited, and (4) Spatial distribution of temperature over the specimen is uniform although temperature variation over time is allowed and has no effect on the proposed technique. A further study is underway to develop a reference-free delamination detection technique, which does not use prior baseline data, comparison of signals among multiple paths or predetermined decision boundary, is underway.

7. ACKNOWLEDGEMENT

This work is supported by the Boeing Company, the Radiation Technology Program (M20703000015-07N0300-01510) and the Nuclear Research & Development Program (2009-0083489) of National Research Foundation of Korea (NRF) funded by Ministry of Education, Science & Technology (MEST).

REFERENCES

- [1] Raghavan, A. and Cesnik, C. E. S., "Review of guided-wave structural health monitoring," *Shock Vib. Dig.* 39, 91–114 (2007).
- [2] Kessler, S. S., Spearing, S. M. and Soutis, C., "Damage detection in composite materials using Lamb wave methods," *Smart Mater. Struct.* 11, 269–278 (2002).
- [3] Giurgiutiu, V. and Cuc, A., "Embedded non-destructive evaluation for structural health monitoring, damage detection, and failure prediction," *Shock Vib. Dig.* 37, 83-105 (2005).
- [4] Su, Z., Ye, L. and Lu, Y., "Guided Lamb waves for identification of damage in composite structures: A review," *J. Sound Vib.* 295,753–780 (2006).
- [5] Ip, K. H. and Mai, Y. W., "Delamination detection in smart composite beams using Lamb waves," *Smart Mater. Struct.* 13, 544-551 (2004).
- [6] Yang, M. and Qiao, P., "Modeling and experimental detection of damage in various materials using the pulse-echo method and piezoelectric sensors/actuators," *Smart Mater. Struct.* 14, 1083-1100 (2005).
- [7] Lestari, W. and Qiao, P., "Application of wave propagation analysis for damage identification in composite laminated beams," *J. Comp. Mater.* 39, 1967-1984 (2005).
- [8] Petculescu, G., Krishnaswamy, S. and Achenbach, J. D., "Group delay measurements using modally selective Lamb wave transducers for detection and sizing of delaminations in composites," *Smart Mater. Struct.* 17, 015007 (2007).
- [9] Ihn, J. B. and Chang, F. K., "Pitch-catch active sensing methods in structural health monitoring for aircraft structures," *Structural Health Monitor* 7, 5-19 (2008).
- [10] Wang, D., Ye, L., Lu, Y. and Su, Z., "Probability of the presence of damage estimated from an active sensor network in a composite panel of multiple stiffeners," *Comp. Sci. Tech.* 69, 2054-2063 (2009).
- [11] Kim, S. B. and Sohn, H., "Instantaneous reference-free crack detection based on polarization characteristics of piezoelectric materials," *Smart Mater. Struct.* 16, 2375-2387 (2007).
- [12] Sohn, H. and Kim, S. B., "Development of dual PZT transducers for reference-free crack detection in thin plate structures," *IEEE Trans. Ultrason. Ferroelectr. Freq. Control* 57, 229-240 (2010).

- [13] Anton, S. R. and Inman, D. J., "Reference-free damage detection using instantaneous baseline measurements," AIAA 47, 1952-1964 (2009).
- [14] Yeum, C. M., Sohn, H. and Ihn, J. B., "Lamb wave mode decomposition using concentric ring and circular piezoelectric transducers," Wave Motion (2010). (doi:10.1016/j.wavemoti.2011.01.001)
- [15] <http://www.metisdesign.com> (date last viewed 2/15/11)
- [16] Hong, J. C., Sun, K. H. and Kim, Y. Y., "The matching pursuit approach based on the modulated Gaussian pulse for efficient guided wave damage detection," Smart Mater. Struct. 14, 548-560 (2005).
- [17] Al-Athari, F. M., "Estimation of the mean of truncated exponential distribution," J. Math Stat. 4(4), 284-288 (2008).